RSC Advances




ROYAL SOCIETY OF CHEMISTRY

www.rsc.org/advances

RSC Advances

RSCPublishing

ARTICLE

# Electrodeposition of Manganese Dioxide Film on Activated Carbon Paper and Application for Supercapacitor with High Rate Capability

Cite this: DOI: 10.1039/x0xx00000x

Received 00th xxxxx 2014,
Accepted 00th xxxxx 2014

DOI: 10.1039/x0xx00000x

www.rsc.org/

Yongfu Qiu,[a] Pingru Xu,[a] Bing Guo,[a] Zhiyu Cheng,*[a] Hongbo Fan,[a] Minlin Yang,[a] Xiaoxi Yang, [a] Jianhui Li [b]

Abstract: In this research Magnesium dioxide ($MnO_2$) is electrodeposited over activated carbon paper (ACP) to form a composited $MnO_2$/ACP material. The as-prepared $MnO_2$/ACP shows excellent capacitance performance with a quite high specifc capacitance of 485.4 F/g calculated from discharge curve with current density 2.0 A/g, owing to its enlarged specific surface area and improved electronic conductivity. Moreover, the $MnO_2$/ACP possesses remarkable rate capability due to the ease access of electrolytic ions, leading to the full utilization of $MnO_2$ active material for surpercapacitors. In a word, the electrodeposition of $MnO_2$ thin film on activated carbon paper is reported for the first time, and the composited $MnO_2$/ACP is a promising electrode material for building up efficient supercapacitor.
Key words: Supercapacitor; Carbon paper; Hummers' method; Electrodoposition; Manganese dioxide

## 1.Introduction

Supercapacitors as energy storage devices have attracted great attention over the past few years due to their fast charge/discharge rates, high power densities, long lifetimes and a good safety record. [1-7] Generally, supercapacitors are classified into electrical doublelayer capacitors (EDLCs) [1, 2] and pseudocapacitors [3-7] on the basis of the different charge storage mechanisms. Compared to EDLCs, pseudocapacitors based on metal oxides or conducting polymers are more attractive because of their higher capacitance and energy density through Faradic reactions [3-7]. Among various pseudocapacitive materials, manganese dioxide ($MnO_2$) has been considered as the most attractive candidate in terms of its superior capacitor performance (the theoretical capacitance 1370 F $g^{-1}$), environment friendly and cost-effective. [8] However, supercapacitors based on $MnO_2$ alone often show poor rate capability owing to its low electrical conductivity ($10^{-5}$ - $10^{-6}$ S $cm^{-1}$) [9, 10]. So far, to maximize utilization of $MnO_2$ pseudocapacity, a lot of efforts have been devoted to growing $MnO_2$ nanostructures on stable carbon substrates, such as graphite, carbon nanotube, reduced graphene oxide, graphene and carbon nano-onion etc. because of their high electrical conductivity and good mechanical strength [11-15].

Herein, carbon papers are used as substrates or current collectors for $MnO_2$ based pseudocapacitors due to their chemical stability in strong acidic solution, highly electronic conductive and cost-effective. [16] However, commercial carbon paper is hydrophobic and generally has low specific surface area, thus appropriate surface chemical modification is required to ensure their wettability and electrochemical activity before utilized as substrate. [17-19] Electrodeposition technique is deemed as an effective route to prepare manganese oxide film on substrates. [15] In this research, the eletrodeposited $MnO_2$ thin film on activated carbon paper ($MnO_2$/ACP) possesses an specific capacitance as high as 485.4 F/g calculated from discharge curve with current density 2.0 A/g. The corresponding values of $MnO_2$/ACP calculated from cyclic votammograms at scan rate 20 and 50 mV/s are 312.0 and 235.2 F/g, respectively, which retain 81.7% and 61.6% of the corresponding value at 10 mV/s (382.0 F/g), implying that the sample $MnO_2$/ACP

possess good rate capability as active electrode material for supercapacitor.

## 2.Experimental

**2.1 Preparation of Activated Carbon paper (ACP):** The commercial carbon papers (CP, purchased from Jixing Sheng An Corp., 1.0 cm×4.0 cm, the thickness 0.30 mm, mass density 32 mg/cm$^2$) were soaked in a solution mixture containing 20 mL of concentrated $H_2SO_4$ (98%) and 2 g of $KMnO_4$ (slowly added into $H_2SO_4$) at 25 ℃ for 120 seconds. Afterward the activated carbon papers were heated at 150 ℃ for 2 h, and then washed with distilled water for three times. This treatment is denoted as a modified hummer's method [20] and the activated carbon paper was abbreviated as ACP in the description below.

**2.2 Preparation of $MnO_2$/Activated Carbon Paper ($MnO_2$/ACP):** The $MnO_2$ film was formed on activated carbon paper by anodic electrochemical deposition in a solution of 0.1 M manganese acetate at 25 $^oC$ for 120 s (0.90 V vs Ag/AgCl). Consequently, the as-deposited $MnO_2$ film on the activated carbon paper was then annealed at 150 $^oC$ for 2.0 h and denoted as $MnO_2$/ACP. For comparison, $MnO_2$ film deposited on the commercial carbon paper was prepared and denoted as $MnO_2$/CP.

**2.3 Charaterization:** The morphologies and elemental microprobe analyses were performed on a JEOL 6701F scanning electron microscopy (SEM) equipped with an INCA PentaFETx3 (Oxford Instruments) energy dispersive X-ray spectroscopy (EDS) detector; the atomic force microscope (AFM) images was obtained on a scanning probe microscope (CSPM5600, Being Nano-Instruments LTD.). The specific surface areas of samples were determined by nitrogen adsorption at 77 K with a JWGB SCI.& TECH BK132F automatic adsorption apparatus; Contact angels were observed from a surface tension meter (Dataphysics OCA20, Germany) at 25 $^oC$.

Cyclic voltammetry (CV) and galvanostatic charge/discharge measurements were performed in a three-electrode system using a CHI 440a electrochemical work station, with 1.0 M $Na_2SO_4$ as the electrolyte solution. As-prepared samples with an area of 1.0 cm$^2$ were used as the working electrode, Ag/AgCl (3.0 M KCl) and a Pt wire as the reference and counter electrodes, respectively. The electrochemical impedance spectroscopy (EIS) measurements were carried out by using a potentiostat (EG&G, M2273), the frequency range analyzed was 0.1 Hz to 100 Hz with ac amplitude of 10 mV.

**2.4 Calculation:** The specific capacitance of the electrode can be calculated according to the following equation [21]: $C = \frac{1}{m\upsilon(U_c-U_a)}\int_{U_a}^{U_c} I(U)dU$, Where C is the specific capacitance (F/g), m is mass of electroactive material (g), υ is the potential scan rate (V $s^{-1}$), $U_c - U_a$ is the sweep potential range of the discharging branch and I(U) denotes the response current density (A/g). Alternatively, gravimetric capacitance for a single electrode was calculated from the discharge curve in a three-electrode cell as, $C_{single} = \frac{I\Delta t}{\Delta V}$ ,Where I is the constant current (A/g), Δt is the discharge time, ΔV is the voltage change during the discharge process.[21]

## 3.Results and Discussion

**3.1 SEM, EDS and AFM:** Figure 1A and 1B are the SEM images of the surface morphologies of CP and ACP. In contrast to that of CP, the surface of ACP turned rough, indicating that its surfaces were changed over the modified hummer's treatment. SEM images of $MnO_2$/CP and $MnO_2$/ACP are shown in Figure 1C and 1D. It was observed that layers of film covered the surfaces of CP and ACP after $MnO_2$ was deposited. Obviously, there are more cracks on the surface of $MnO_2$/ACP as compared to that of $MnO_2$/CP. In order to detect the composition of the film, EDS profile was collected and shown in Figure 1E. It was clearly revealed that the film is composed of Mn and O with a ratio of about 1 : 2, which is consistent with the chemical formula of $MnO_2$. AFM results in Figure 1F shows that the thickness of the $MnO_2$ film are about 0.58 ~ 1.25 μm. The mass loadings of the $MnO_2$ for $MnO_2$/CP and $MnO_2$/ACP are 0.48 and 0.51 mg/cm$^2$.

### 3.2 $N_2$ Adsorption-desorption and XRD

In Figure 2A nitrogen adsorption-desorption measurement were performed to examine surface properties of samples. The sharp increase in the $N_2$ adsorbed quantity near the relative pressure $P/P_o$ of 1 indicates only the macropores exist in the samples ACP and $MnO_2$/ACP. According to the Brunauner-Emmett-Teller (BET) analysis, the specific surface areas for ACP and $MnO_2$/ACP are 21.1 and 7.7 $m^2$/g. The specific surface area for $MnO_2$/ACP is lower than that of ACP due to the rough surface was covered by a thin layer $MnO_2$.

The crystalline structures of ACP and $MnO_2$/ACP were characterized by powder X-ray diffraction (XRD) and the results are shown in Figure 2B. The XRD pattern a for ACP in Figure 2B is ascribed to carbon (PDF#12-0212) with lattice constants of a = 0.2464 nm and c = 0.6736 nm. In addition to the two peaks at 2θ = 26.4 and 54.5 $^o$ for carbon, another two diffraction peaks at 2θ = 36.8 and 65.7 $^o$ indexed to $MnO_2$ birnessite structure (PDF#18-0802, lattice constants a = 0.5820 nm and c = 0.1462 nm) in pattern b were observed. The grain diameter of the $MnO_2$ on ACP can be calculated using Scherrer's equation [22] $D = \frac{0.9\lambda}{\beta \cos\theta}$, where β is the broadening of diffraction line measured at half maximum intensity (radians) and λ= 0.154056 nm, the wavelength of the Cu $K_a$ X-ray. The grain diameter of the $MnO_2$ in the film was calculated to be 6.8 nm.

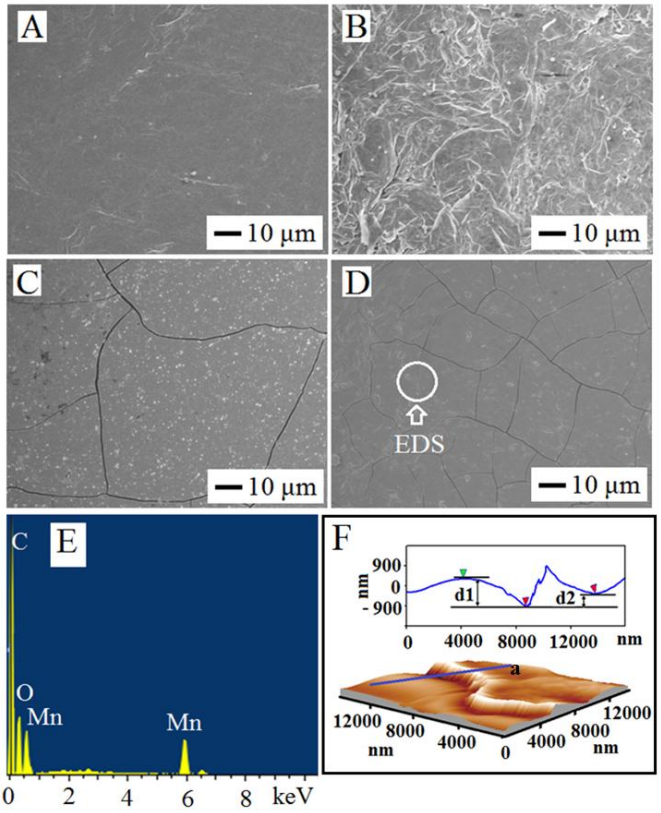


**Figure 1.** SEM images of: (A)CP; (B)ACP; (C)$MnO_2$/CP; (D)$MnO_2$/ACP; (E) EDS profile of the $MnO_2$ film shown in the marked area by cycle in (D); and F) AFM image of $MnO_2$/ACP (down), and the profile of the topography with scan line **a** (up).

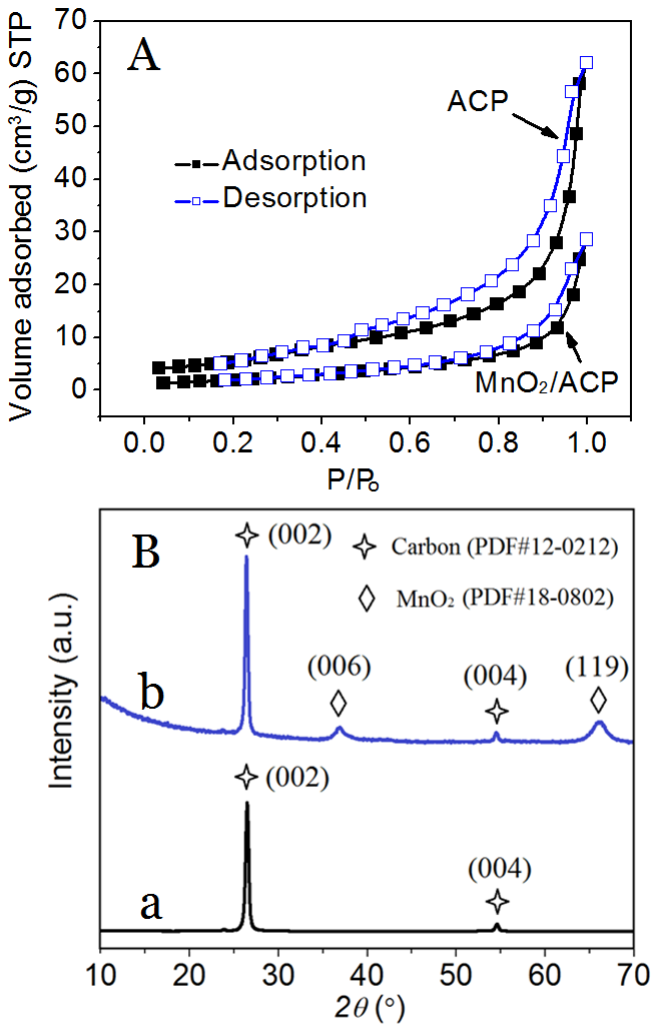


**Figure 2.** (A) $N_2$ adsorption-desorption isotherms; (B) XRD patterns of (a) ACP; (b) $MnO_2$/ACP.

### 3.3 Wetting Property:

The wetting property of the sample was characterized by water contact angle test. [23] The contact angle is the angle measured through the liquid, where a liquid/vapor interface meets a solid surface, which quantifies the wettability of a solid surface by a liquid via the Young equation:[23] $0 = \gamma_{SG} - \gamma_{SL} - \gamma_{LG}\cos\theta_C$, where, $\gamma_{SG}$ is the solid–vapor interfacial energy, $\gamma_{SL}$ as the solid–liquid interfacial energy, $\gamma_{LG}$ as the liquid–vapor interfacial energy and $\theta_C$ is the equilibrium contact angle. Generally, if the water contact angle is smaller than 90°, the solid surface is considered as hydrophilic. The contact angles of water droplets on the surface of CP, ACP, $MnO_2$/CP and $MnO_2$/ACP are shown in Figure 3. Obviously, the contact angle $72.0 \pm 0.3^o$ for ACP is smaller than that of CP $117.0 \pm 0.5^o$, indicating that the surface hydrophilicity is enhanced over the modified hummer's treatment. This enhancement could be ascribed to the hydrophilic groups such as hydroxyl (—OH), carbonyl (>C=O) and carboxyl (—COOH) introduced into the surface of carbon papers and they act as strong polar sites that absorb water molecules. [24] Further, the contact angles for $MnO_2$/CP and $MnO_2$/ACP are $49.5 \pm 0.5^o$ and $42.0 \pm 0.5^o$, both lower than those of their counterparts, suggesting that the intake of $MnO_2$ bring enhanced hydrophilicity to both CP and ACP.

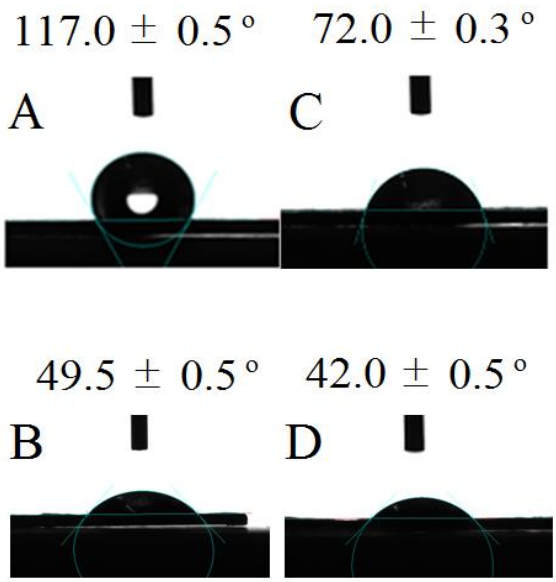


**Figure 3.** Cross-sectional views of water droplets on (A) CP; (B) $MnO_2$/CP and (C) ACP; (D) $MnO_2$/ACP.

### 3.4 Cyclic Voltammetry and Galvanostatic Charge/discharge Measurements:

The electrochemical performance of as-prepared samples were investigated in a three-electrode system, in which 1.0 M $Na_2SO_4$ was used as electrolyte, as-prepared samples as working electrode, Ag/AgCl and Pt wire as the reference and counter electrodes, respectively. [25] The cyclic votammograms collected at different scan rates for the samples are shown in Figure 4. From Figure 4A to 4D, it was obvious that the enclosing areas of the CV curves increase with the increasing potential scan rates and the specific capacitance could be calculated from CV curves using the equation [21]:$C = \frac{1}{m\upsilon(U_c - U_a)}\int_{U_a}^{U_c} I(U)dU$. The calculated specific capacitances of samples under 10 mV/s are shown in Figure 4F. The corresponding

values for CP and ACP are 113.0 and 158.6 F/g, while those for $MnO_2$/CP and $MnO_2$/ACP are 326.8 and 382.0 F/g, suggesting that loading $MnO_2$ thin films on CP or ACP have dramatically increased the specific capacitances. In Figure 4E, the enlarged CV diagrams for $MnO_2$/CP and $MnO_2$/ACP show quasi-rectangular shapes as the typical signature of the ideal capacitive materials, exhibiting their good electrochemical behaviors. Furthermore, the specific capacitance 382.0 F/g for $MnO_2$/ACP is higher than that for $MnO_2$/CP 326.8 F/g, implying that the activated surface of carbon paper has remarkable affects on the electrochemical behaviors of the composited electrodes, which owing to the enlarged specific surface area and the improved hydrophilicity.

The rate capabilities of electrode materials could also be reflected by the CV curves at different scan rates shown in Figure 4. These CV curves exhibit rectangular shapes at low scan rates (< 100 mV/s), and they clearly deviate from rectangular shapes at increased scan rate (> 100 mV/s). This could be explained by the relatively slow diffusion of $Na^+$ within the $MnO_2$ matrix [27, 28] and accordingly the $MnO_2$ materials under the interface did not actively contribute to the performance of seudocapacitance. The specific capacitances of $MnO_2$/ACP calculated from cyclic votammograms at scan rates of 20 and 50 mV/s are 312.0 and 235.2 F/g, which retain 81.7% and 61.6% of the corresponding value at 10 mV/s (382.0 F/g), implying that the sample $MnO_2$/ACP possess better rate capability as active electrode material for supercapacitor rather than others.

The $MnO_2$/ACP exhibits the best supercapacitor performance, as further confirmed by the galvanostatic charge/discharge measurements in a three-electrode system. Figure 5A shows the charge-discharge curves for $MnO_2$/ACP at different current densities. These curves generally show symmetrical and linear profiles, indicating that $MnO_2$/ACP has excellent supercapacitive behavior. The specific capacitances for a single electrode calculated from the discharge branch are shown in Figure 5B. [21] When the current densities are 2.0, 4.0, 6.0, 8.0, 10.0 and 12.0 A/g, the corresponding specific capacitances of 485.4, 397.2, 336.8, 295.4, 265.0 and 237.8 F/g could be observed, suggesting that superior reversible redox reactions take place within $MnO_2$/ACP, leading to its excellent supercapacitive behavior. The specific capacitance for $MnO_2$/ACP is 295.4 F/g at current density 10 A/g, which is higher than 250.0 F/g for the flat $MnO_2$ electrode and lower than 714.1 F/g for three-dimensional Au/$MnO_2$ nanocone arrays electrode. [29]

Good capacitance retention is crucial for practical supercapacitors,. [29] The capacitance retention test over 2000 cycles for $MnO_2$/ACP was performed at a current density of 20 A/g and the results are shown in Figure 6A. A capacitance decay over 2000 cycles is ~15%, indicating its excellent long-term capacitive stability.

To further study the resistant of the supercapacitror in the CP and ACP electrodes, electrochemical impedance spectroscopy (EIS) were collected and shown in Figure 6B. The Nyquist-type impedance spectra for ACP and $MnO_2$/ACP electrodes in Figure 6B contain only upward sloping lines, indicating that both electrodes have low diffusion resistance and exhibit good capacitive performance. [30, 31]

In order to design high performance supercapacitors, several factors have to be considered. In our case, electronic conductivity of the composited $MnO_2$/ACP and taking electrochemical advantage of $MnO_2$ material are important. First, considering that the electronic conductivity of $MnO_2$/ACP largely depend on the surface structure of ACP and the interaction between the $MnO_2$ film and ACP, the carbon paper was firstly treated by the modified hummer's method to improve its hydrophilicity such to enhance its interaction with the deposited $MnO_2$. Second, very thin $MnO_2$ film deposited on the ACP makes electrolytic ions easily access to the active material, so that full advantage of $MnO_2$ as electrode active material for surpercapacitor could be realized. In a word, the electrodeposition of $MnO_2$ thin film on activated carbon paper ($MnO_2$/ACP) is reported for the first time, and the composited $MnO_2$/ACP is deemed as a promising electrode material for building up efficient supercapacitors.

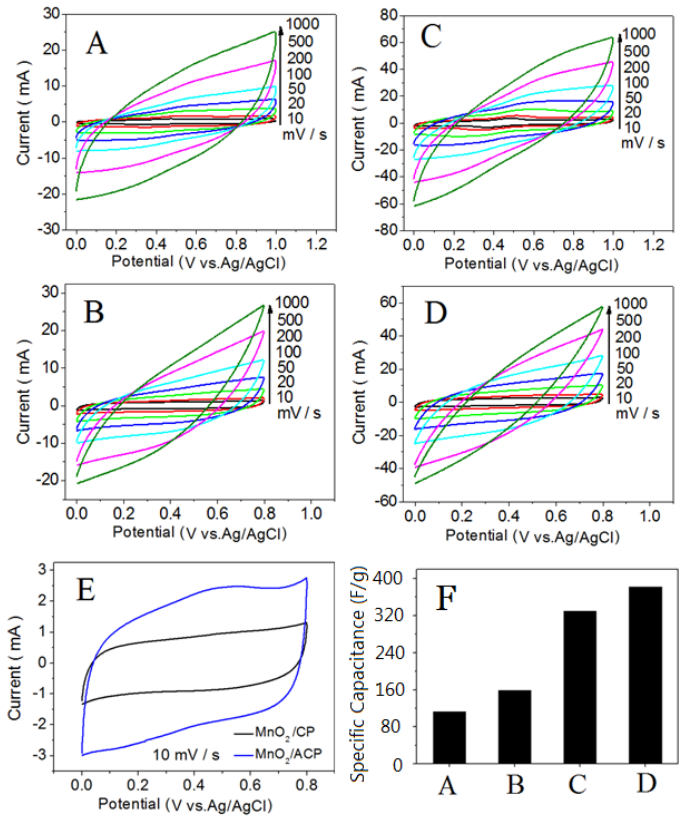


**Figure 4.** Cyclic votammograms collected at different scan rates for: (A) CP; (B) $MnO_2$/CP ; (C) ACP and (D) $MnO_2$/ACP; E) Enlarged CV diagrams for $MnO_2$/CP and $MnO_2$/ACP at scan rate 10 mV/s; (F) Calculated specific capacitances of the samples from plot A ~D at scan rate 10 mV/s.

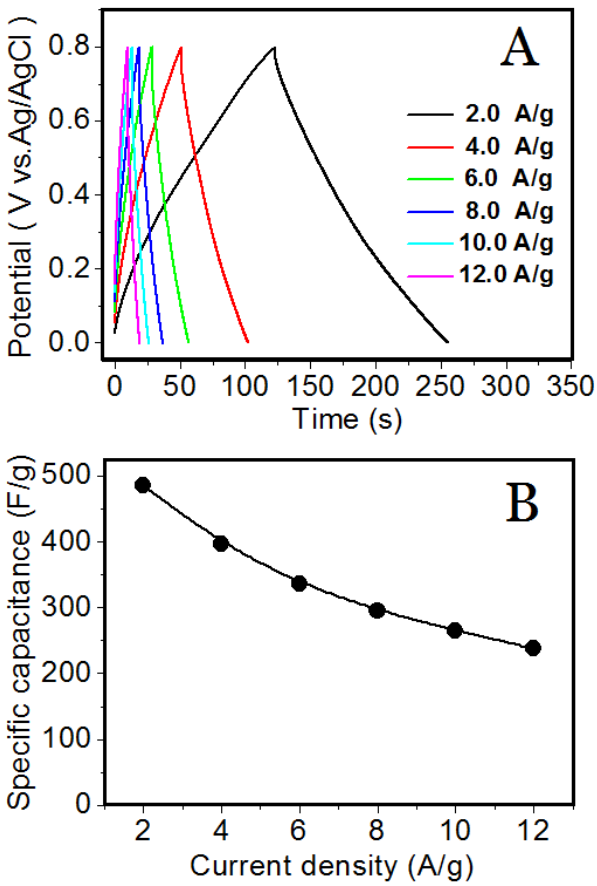


**Figure 5.** (A) Charge-discharge curves at various current densities for $MnO_2$/ACP; (B) Specific capacitance calculated based on charge-discharge curves from plot (A) as a function of current density.

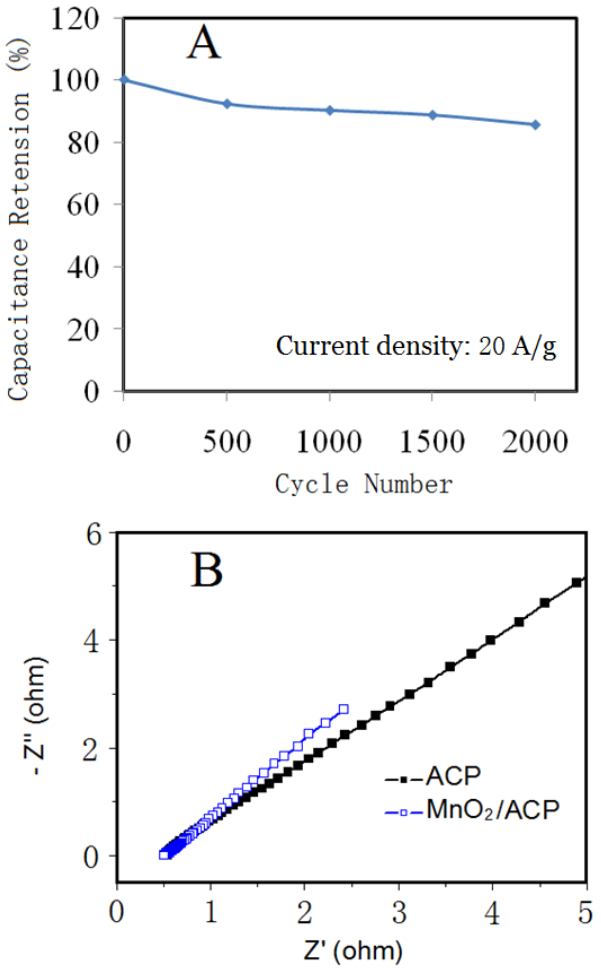


**Figure 6.** (A) Capacitance retention test over 2000 cycles at a current density of 20 A/g for $MnO_2$/ACP; (B) Nyquist electrochemical impedance spectra for ACP and $MnO_2$/ACP.

## 4. Conclusion

In summary, Magnesium dioxide ($MnO_2$) electrodeposited over activated carbon paper (ACP) to form a composited $MnO_2$/ACP material was prepared and characterized by the SEM, EDS, AFM, XRD and contact angle testing. Further, the supercapacitive behaviors of samples were measured by the cyclic voltammetry (CV) and galvanostatic charge/discharge. The as-prepared $MnO_2$/ACP shows excellent capacitance performance with a quite high specific capacitance of 485.4 F/g calculated from discharge curve with current density 2 A/g, owing to its enlarged specific surface area and improved electronic conductivity. Moreover, the specific capacitances of $MnO_2$/ACP obtained from cyclic votammograms at scan rates of 20 and 50 mV/s are 312.0 and 235.2 F/g, which retain 81.7% and 61.6% of the corresponding value at 10 mV/s (382.0 F/g), implying that the sample $MnO_2$/ACP possess better rate capability as active electrode material for supercapacitor rather than others due to the ease access of electrolytic ions, leading to the full utilization of $MnO_2$ active material for surpercapacitors. In a word, the electrodeposition of $MnO_2$ thin film on activated carbon paper ($MnO_2$/ACP) is reported for the first time, and the composited $MnO_2$/ACP is a promising electrode material for building up efficient supercapacitor.

## Acknowledgements

The work described in this paper was supported by the National Natural Science Foundation of China (No. 51206029)

## Notes and references

[a] *College of Chemistry and Environmental Engineering and Guangdong Provincial Key Laboratory of Distributed Energy Systems, Dongguan University of Technology, Guangdong 523808, P. R. China.*

[b] *National Engineering Laboratory for Green Chemical Productions of Alcohols–Ethers –Esters, College of Chemistry and Chemical Engineering, Xiamen University, Xiamen, 361005, China.*

**Author to whom any correspondence should be addressed. Tel/fax: +86 769 2286 1232, E-mail address: mszycheng@scut.edu.cn or qiuyf1979@foxmail.com.*

1 P. Simon and Y. Gogotsi, *Nat. Mater.*, 2000, **91**, 845-854.

2 A. Burke, *J. Power Sour.*, 2000, **91**, 37-50.

3 J. P. Zheng, P. J. Cygan and T. R. Jow, *J. Electrochem. Soc.*, 1995, **142**, 2699-2703.

4 M. H. Yu, T. Zhai, X. H. Lu, X. J. Chen, S. L. Xie, W. Li, C. L. Liang, W. X. Zhao, L. P. Zhang and Y. X. Tong, *J. Power Sour.*, 2014, **239**, 64-71.

5 S. C. Pang, M. A. Anderson and T. W. Chapman, *J. Electrochem. Soc.*, 2000, **147**, 444-450.

6 H. M. Lee, K. T. Lee and C. K. Kim, *Materials*, 2014, **7**, 265-

274.

7 S. J. He, C. X. Hu, H. Q. Hou and W. Chen, *J. Power Sour.*, 2014, **246**, 754-761.

8 Z. B. Lei, J. T. Zhang and X. S. Zhao, *J. Mater. Chem.*, 2012, **22**, 153-160.

9 S. W. Lee, J. Kim, S. Chen, P. T. Hammond and Y. Shao-Horn, *Acs Nano*, 2010, **4**, 3889-3896.

10 F. Cao, Y. M. Liu, B. L. Chen, L. F. Fei, Y. Wang and J. K. Yuan, *Electrochim. Acta*, 2012, **81**, 1-7.

11 G. P. Xiong, K. P. S. S. Hembram, R. G. Reifenberger and T. S. Fisher, *J. Power Sour.*, 2013, **227**, 254-259.

12 X. Zhao, L. L. Zhang, S. Murali, M. D. Stoller, Q. H. Zhang, Y. W. Zhu and R. S. Ruoff, *ACS Nano*, 2012, **6**, 5404-5412.

13 B. G. Choi, Y. S. Huh, W. H. Hong, H. J. Kim and H. S. Park, *Nanoscale*, 2012, **4**, 5394-5400.

14 D. Y. Zhai, B. H. Li, H. D. Du, G. Y. Gao, L. Gan, Y. B. He, Q. H. Yang and F. Y. Kang, *Carbon*, 2012, **50**, 5034-5043.

15 D. K. Walanda, G. A. Lawrance and S. W. Donne, *J. Power Sour.*, 2005, **139**, 325-341.

16 M. H. Chakrabarti, N. P. Brandon, S. A. Hajimolana, F. Tariq, V. Yufit, M. A. Hashim, M. A. Hussain, C. T. J. Low and P. V. Aravind, *J. Power Sour.*, 2014, **253**, 150-166.

17 B. Sun and M. Skyllas-Kazacos, *Electrochim. Acta.*, 1992, **37**, 1253-1260.

18 L. Yue, W. Li, F. Sun, L. Zhao and L. Xing, *Carbon*, 2010, **48**, 3079-3090.

19 X. X. Wu, H. F. Xu, P. C. Xu, Y. Shen, L. Lu, J. C. Shi, J. Fu and H. Zhao, *J. Power Sour.*, 2014, **263**, 104-109.

20 W. S. Hummer and R. E. Offeman, *J. Am. Chem. Soc.*, 1958, **80**, 1339-1339.

21 J. Yan, Z. J. Fan, T. Wei, J. Cheng, B. Shao, K. Wang, L. P. Song and M. L. Zhang, *J. Power Sour.*, 2009, **194**, 1202-1207.

22 O. Durupthy, J. Bill and F. Aldinger, *Cryst. Growth Des.*, 2007, **7**, 2696-2704.

23 T. S. Chow, *J. Phys.: Condens. Matter*, 1998, **10**, L445-L451.

24 N. Giovambattista, P. G. Debenedetti and P. J. Rossky, *J. Phys. Chem. B*, 2007, **111**, 9581-9587.

25 Y. Shi, L. J. Pan, B. R. Liu, Y. Q. Wang, Y. Cui, Z. A. Bao, G. H. Yu, *J. Mater. Chem. A*, 2014, **2**, 6086-6091.

26 F. Yang, J.Y. Yao, F.L. Liu, H.C. He, M. Zhou, P. Xiao, Y.H. Zhang, *J. Mater. Chem. A*, 2013, **1(3)**: 594-601.

27 S. M. Zhu, H. S. Zhou, M. Hibino, I. Honma and M. Ichinara, *Adv. Funct. Mater.*, 2005, **15**, 381-386.

28 R. K. Sharma, H. S. Oh, Y. G. Shul and H. Kim, *Physica B.*, 2008, **403**, 1763-1769.

29 Y. C. Qiu, Y. H. Zhao, X. W. Yang, W. F. Li, Z. H. Wei, J. W. Xiao, S. F. Leung, Q. F. Lin, H. K. Wu, Y. G. Zhang, Z. Y. Fan, S. H. Yang, *Nanoscale*, 2014, **6**, 3626-3631.

30 C. W. Huang, C. A. Wu, S. S. Hou, *Adv. Funct. Mater.*, 2012, **22**, 4677-4685.

31 Z. Gui, H. L. Zhu, E. Gillette, *ACS Nano*, 2013, **7**, 6037-6046.

# Elecrodeposition of Manganese Dioxide Film on Activated Carbon Paper and Application for Supercapacitor with High Rate Capability

Yongfu Qiu, [a] Pingru Xu, [a] Bing Guo,[a] Zhiyu Cheng,*[a] Hongbo Fan,[a] Minlin Yang, [a] Xiaoxi Yang, [a] Jianhui Li[b]

[a] *College of Chemistry and Environmental Engineering and Guangdong Provincial Key Laboratory of Distributed Energy Systems, Dongguan University of Technology, Guangdong 523808, P. R. China.*

[b] *National Engineering Laboratory for Green Chemical Productions of Alcohols–Ethers – Esters, College of Chemistry and Chemical Engineering, Xiamen University, Xiamen, 361005, China.*

**Author to whom any correspondence should be addressed. Tel/fax: +86 769 2286 1232, E-mail address: mszycheng@scut.edu.cn; qiuyf1979@foxmail.com.*

**Table of Content**

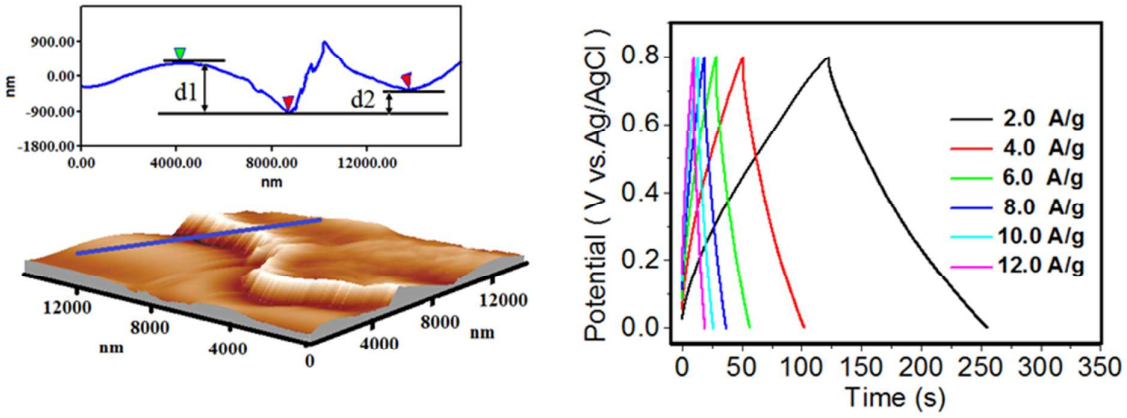


The composited $MnO_2$/ACP is reported for the first time and it shows high specific capacitance and remarkable rate capability.